Fibroblast activation protein restrains adipogenic differentiation and regulates matrix-mediated mTOR signaling

Rachel Blomberg[a], **Daniel P. Beiting**[b], **Martin Wabitsch**[c] and **Ellen Puré**[a]

a - Department of Biomedical Sciences, University of Pennsylvania School of Veterinary Medicine, Philadelphia, PA, United States of America
b - Department of Pathobiology, University of Pennsylvania School of Veterinary Medicine, Philadelphia, PA, United States of America
c - Department of Pediatrics and Adolescent Medicine, University Medical Center Ulm, Germany

Correspondence to Ellen Puré: 380 S. University Ave, Philadelphia, PA 19104, United States of America.
epure@upenn.edu
https://doi.org/10.1016/j.matbio.2019.07.007

Abstract

Obesity is a risk factor for multiple diseases, including diabetes, cardiovascular disease, and cancer. Within obese adipose tissue, multiple factors contribute to creating a disease-promoting environment, including metabolic dysfunction, inflammation, and fibrosis. Recent evidence points to fibrotic responses, particularly extracellular matrix remodeling, in playing a highly functional role in the pathogenesis of obesity. Fibroblast activation protein plays an essential role in remodeling collagen-rich matrices in the context of fibrosis and cancer. We observed that FAP-null mice have increased weight compared to wild-type controls, and so investigated the role of FAP in regulating diet-induced obesity. Using genetically engineered mouse models and *in-vitro* cell-derived matrices, we demonstrate that FAP expression by pre-adipocytes restrains adipogenic differentiation. We further show that FAP-mediated matrix remodeling alters lipid metabolism in part by regulating mTOR signaling. The impact of FAP on adipogenic differentiation and mTOR signaling together confers resistance to diet-induced obesity. The critical role of ECM remodeling in regulating obesity offers new potential targets for therapy.

Introduction

Obesity is a growing epidemic in the modern world. In the United States, over one-third of all adults are categorized as obese, as measured by body mass index [1]. Obesity can have profound systemic effects, and is a risk factor for multiple diseases, including diabetes, cardiovascular disease, and various cancers. These sequelae may be due to a combination of systemic effects of obesity, such as metabolic dysfunction, hypertension, and widespread inflammation [2]. In obesity, adipocytes undergo both hyperplasia and hypertrophy, and display enhanced secretion of mitogenic and pro-inflammatory adipokines. Inflammatory macrophages are recruited to and active within obese adipose, and vascularization is dysregulated [3]. Obese adipose also displays hallmarks of fibrosis, including increased fibroblast activation and excessive accumulation of extracellular matrix (ECM) [4].

Emerging evidence indicates that this fibrotic response is not merely a result of obesity, but in fact plays a critical role in regulating adipocyte biology [5]. In rodent models, experimental manipulation of various ECM components and matrix remodeling enzymes can result in impaired adipogenesis and/or reduced adipocyte hypertrophy—phenotypes typically associated with improved metabolic health [6–9]. Multiple studies have implicated hyaluronan and its most common receptors, CD44 and RHAMM, in regulating adipogenesis and thereby disorders like insulin resistance and diabetes [10]. Similarly, mice lacking longer isoforms of collagen XVIII showed reduced adiposity along with reduced collagen XVIII specifically in the adipocyte pericellular space. *In vitro* studies indicate that the longer isoforms of collagen XVIII promote the maintenance of pre-adipocyte populations and contribute to inhibition of Wnt signaling, thereby allowing adipogenesis to proceed [11]. Conversely,

the extracellular protease Adamts1 inhibits adipocyte lineage commitment. Silencing of Adamts1 promotes weight gain and metabolic syndrome in mice as well as expression of various ECM proteins including collagen I. *In vitro* experiments suggest that loss of Adamts1 attenuates FAK/ERK signaling, and that this contributes to enhanced adipogenic lineage commitment [12]. Collectively, these studies indicate that ECM can play a role in regulating obesity and the metabolic symptoms commonly associated with weight gain.

Intriguingly, some studies suggest that ECM may be a critical link between adipocyte biology and systemic metabolism, and that disrupting this link may result in 'metabolically healthy' obesity. *Ob/ob* mice deficient in collagen VI— a major adipose ECM component—display a less dense adipose collagen architecture and more hypertrophic adipocytes than wild-type mice. Despite this increased hypertrophy, the knockout mice show reduced overall body weight and improved glucose tolerance [13]. Additional studies implicate not only total collagen VI levels, but also production of its bioactive cleavage product endotrophin, in regulating systemic metabolism and obesity [14]. Similarly, mice deficient in factor XIII-A transglutimase have reduced overall levels of collagen and fibronectin in their adipose tissue, along with enhanced adipocyte hypertrophy. Yet again, these mice show blunted weight gain and improved insulin sensitivity when fed a high-fat diet [15]. These studies posit that reduced fibrosis allows for adipocyte growth without biomechanical or metabolic stress, thus resulting in better systemic health.

Fibroblast activation protein (FAP) is an ECM-remodeling protease that has gained notoriety in cancer research. Enzymatically, FAP is closely related to other members of the dipeptidyl peptidase (DPP) family of S9 serine proteases, but is unique in also possessing endopeptidase activity [16]. In the context of cancer, FAP plays various pro-tumorigenic roles [17]. In the course of studying the role of FAP in cancer and cardiovascular disease in our laboratory, we noted a recurring pattern that FAP-null mice exhibit an increase in body weight relative to age and sex matched wild-type controls in multiple genetically diverse strains. Interestingly, in diet-induced obese mice, inhibition of DPPIV—FAP's closest molecular relative—has recently been noted to reduce serum triglycerides and cholesterol, as well as improve glucose tolerance, though no effect was observed on adipocyte size or overall body weight [18]. Based on our observations in various mouse models, and the evidence that ECM dynamics may play critical roles in mediating the phenotypes of obesity, we investigated whether FAP can play a role in restraining obesity, particularly through its ECM-remodeling activity. Using genetically engineered mouse models and *in vitro* cell-derived matrices, we demonstrated that loss of FAP results in increased adiposity due, at least in part, to enhanced adipogenic differentiation and matrix-induced adipocyte hypertrophy *via* mTOR signaling.

Results

FAP deletion promotes obesity

In the course of establishing diet-induced obesity models for breast cancer, we placed female FVB mice, $FAP^{+/+}$ and $FAP^{-/-}$, on isocaloric low- and high-fat diets (LFD, HFD) for 18 weeks beginning at 12 weeks of age (Fig. 1A). As expected, HFD caused a significant increase in body mass of $FAP^{+/+}$ mice by the time of analysis at 30 weeks of age. Unexpectedly, we found that $FAP^{-/-}$ mice maintained on LFD showed a comparable increase in body mass to $FAP^{+/+}$ mice maintained on HFD. Moreover, $FAP^{-/-}$ mice on HFD showed a markedly exacerbated weight gain (Fig. 1B) compared to $FAP^{+/+}$ mice on HFD. A similar pattern was observed in isolated subcutaneous fat (Fig. 1C) and, to a lesser degree, visceral fat (Fig. 1D), suggesting that FAP deletion enhanced obesity. These phenotypes occurred in the absence of differences in overall food intake (Fig. S1A).

To address if this weight gain was accompanied by the classical metabolic hallmarks of obesity, we first tested for insulin resistance. 30-week-old mice were fasted for 8 h and then given a bolus injection of 1 U/kg insulin, after which levels of blood glucose were monitored for 120 min. There were no differences in fasted glucose levels between groups (Fig. S1B). We also found no significant differences in insulin response between any of the groups, which may partially be a feature of the female FVB mice we used in our experiments (Fig. 1E). To expand on this metabolic study, we then performed a glucose tolerance test, measuring blood glucose following an injection of 2 g/kg (20% dextrose) glucose. Here we did note that HFD-fed $FAP^{+/+}$ mice showed impaired ability to regulate glucose response, but $FAP^{-/-}$ mice, despite their greater body mass, did not exhibit further impaired glucose tolerance (Fig. 1F). Interestingly, when we measured serum triglyceride levels, we noted that $FAP^{-/-}$ mice on LFD had greater baseline levels of triglycerides than $FAP^{+/+}$ mice on LFD, but that $FAP^{-/-}$ mice on HFD did not display significantly different serum triglyceride levels than normal lean mice (Fig. 1G), perhaps indicating activation of a compensatory mechanism to maintain normal systemic metabolism. Altogether, these data indicate that $FAP^{-/-}$ mice, despite showing increased weight gain, do not also display impaired systemic metabolism.

FAP deletion promotes adipocyte hypertrophy

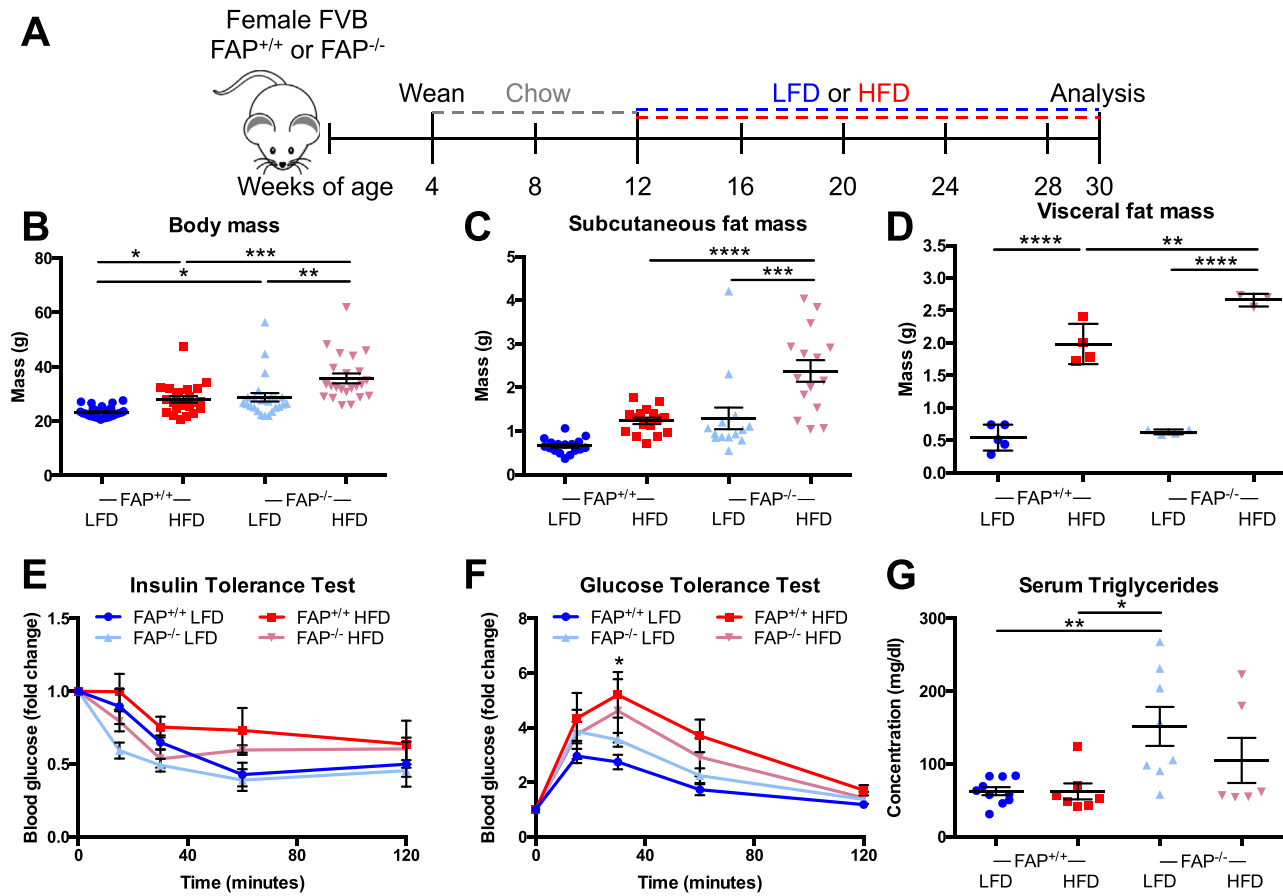We next investigated local microenvironmental changes to subcutaneous adipose tissue, including

Fig. 1. *FAP$^{-/-}$ mice display enhanced diet-induced weight gain with minimal changes to systemic metabolism.* A) Timeline for diet-induced obesity model. B) Total body mass at time of euthanasia, 30 weeks of age ($N = 23-27$ mice/group). C) Mass of total subcutaneous fat at 30 weeks of age ($N = 14-17$ mice/group). D) Mass of total abdominal fat at 30 weeks of age ($N = 3-5$ mice/group) E) Blood glucose levels following bolus insulin injection (1 U/kg body mass; $N = 4-6$ mice/group). F) Blood glucose levels following bolus glucose injection ($p < 0.05$ between FAP$^{+/+}$ LFD and FAP$^{+/+}$ HFD by area under the curve; N = 4−6 mice/group) G) Serum triglyceride levels at 30 weeks of age ($N = 6-10$ mice/group). Statistical analysis by two-way ANOVA.
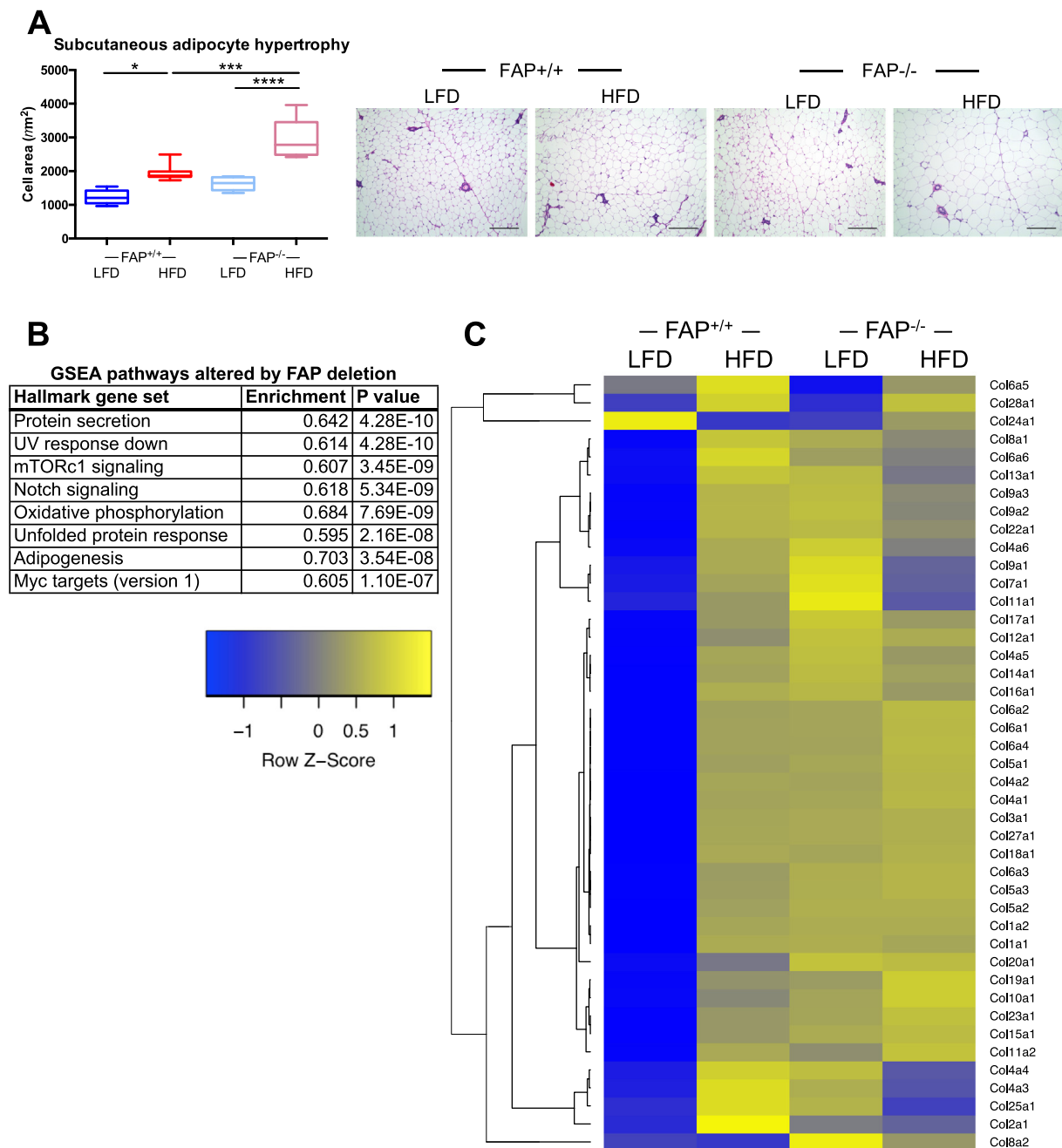
A

B

GSEA pathways altered by FAP deletion

Hallmark gene set	Enrichment	P value
Protein secretion	0.642	4.28E-10
UV response down	0.614	4.28E-10
mTORc1 signaling	0.607	3.45E-09
Notch signaling	0.618	5.34E-09
Oxidative phosphorylation	0.684	7.69E-09
Unfolded protein response	0.595	2.16E-08
Adipogenesis	0.703	3.54E-08
Myc targets (version 1)	0.605	1.10E-07

C

Fig. 2. $FAP^{-/-}$ *mice display enhanced adipocyte hypertrophy and obesity-related gene expression.* A) Subcutaneous fat adipocyte hypertrophy measured in H&E stained sections (scale bar $=200\,\mu m$; N $= 6-10$ mice/group, 10 images/mouse). B) GSEA hallmark pathways that are significantly altered by FAP deletion (regardless of diet). C) Heatmap of RNA levels of all collagen genes as measured by RNAseq (N $= 2-3$ mice/group). Statistical analysis by two-way ANOVA.

addressing whether the gain in fat mass was due to adipocyte hyperplasia, hypertrophy, or both. While we noted trends towards increased adipocyte numbers (Fig. S2A), the most remarkable impact was found to be on adipocyte size. HFD induced adipocyte hypertrophy in both $FAP^{+/+}$ and $FAP^{-/-}$ mice as expected, but the effect was markedly more pronounced in $FAP^{-/-}$ mice, where HFD produced

adipocytes up to three times the size of those in LFD-fed $FAP^{-/-}$ mice (Fig. 2A). A similar, but less pronounced hypertrophy phenotype was seen in abdominal white fat of HFD-fed mice; in contrast, there were no overt differences in intrascapular brown fat, indicating that the adipocyte hypertrophy associated with FAP-deletion was a white fat phenotype selectively (Fig. S2B,C).

We next asked if the mechanisms underlying the subcutaneous adipocyte hypertrophy were cell-intrinsic or extrinsic. To gain an unbiased global perspective, we performed RNAseq on total subcutaneous adipose RNA. Gene set enrichment analysis (GSEA)—a widely used and publically available analysis software for determining differences in coordinated gene networks [19]—demonstrated that FAP deletion alone altered several gene networks commonly associated with obesity, including mTOR signaling and adipogenesis (Fig. 2B). This suggests either that representation of cell populations shifts within the microenvironment, or that cell-intrinsic mechanisms underlie the adipocyte hypertrophy/hyperplasia observed in FAP$^{-/-}$ mice; data presented below support the latter explanation. We also performed GSEA on the matrisome-associated gene sets published by the Matrisome Project [20], which revealed that FAP deletion regulates RNA levels of various ECM components, but most significantly collagens, with expression levels of almost all collagens increased both by HFD and by FAP deletion (Fig. 2C). These ECM alterations suggest that the adipocyte phenotype was potentially reflective of cell-extrinsic mechanisms as well.

FAP is expressed on pre-adipocytes and down-regulated upon adipogenic differentiation

In considering potential cell-intrinsic mechanisms that might contribute to the adipocyte hypertrophy associated with FAP deletion, we first isolated primary murine adipose stromal cells (ASCs) from the subcutaneous fat of FAP$^{+/+}$ and FAP$^{-/-}$ FVB mice. ASCs are a heterogeneous population of mesenchymal cells, most prominently fibroblasts and pre-adipocytes. To assess if FAP$^{+/+}$ and FAP$^{-/-}$ mice simply have different proportions of pre-adipocytes or fibroblasts in subcutaneous fat, we analyzed the expression of various cell lineage markers. Following isolation based on adherence, we found that ASCs from both FAP$^{+/+}$ and FAP$^{-/-}$ mice express high levels of the myofibroblast marker αSMA (relative to HPRT), with no differences between genotype (Fig. S3A). Both genotypes of ASCs also expressed similar levels of PPARγ, though in this case overall levels were low, as expected for pre-adipocytes (Fig. S3B). We also quantified expression of Zfp423, a marker of very early adipogenic commitment, and found no differences in expression of this marker between FAP$^{+/+}$ and FAP$^{-/-}$ ASCs (Fig. 3E). Together, these data indicated that ASCs from FAP$^{+/+}$ and FAP$^{-/-}$ mice have comparable populations of various mesenchymal cell types.

We then sought to determine whether pre- and/or mature adipocytes express FAP. As both fibroblasts and mesenchymal stem cells can express FAP [21], we hypothesized that the related adipocyte lineage could as well. We first addressed this question by isolating ASCs from the subcutaneous fat of FAP$^{+/+}$

FVB mice, and then differentiating them *in vitro* with adipogenic stimuli. Interestingly, while undifferentiated ASCs expressed FAP, we found that upon differentiation, FAP expression was down-regulated (Fig. 3B), indicating that pre- adipocytes can express FAP, but that this expression was lost during differentiation into mature adipocytes. Importantly, these data obtained with murine cells is consistent with a data set recently published by Ehrlund et al. [22] of cell markers from human adipose samples. We mined this data set to discover that FAP is a marker significantly enriched on CD45-CD31-CD34+ adipocyte progenitors over mature adipocytes (Fig. 3C). Additionally, using the pre-adipocyte cell line SGBS, we demonstrated that *in vitro* adipogenic differentiation also reduces FAP expression by human cells (Fig. 3D).

FAP deletion enhances adipogenic differentiation

Based on the RNAseq data presented above (Fig. 2B), we hypothesized that FAP might play a role in adipogenic differentiation. To test this hypothesis, we isolated ASCs from FAP$^{+/+}$ and FAP$^{-/-}$ mice and compared their *in vitro* differentiation. ASCs were seeded onto cell-derived matrices, based on prior data that substratum of physiologically relevant stiffness and composition is necessary to support FAP expression [23], and then treated with a cocktail of insulin, dexamethasone, and IBMX (Fig. 4A). Following adipogenic differentiation, we assessed PPARγ expression and overall lipid accumulation *via* oil-red-O (ORO) staining. FAP$^{-/-}$ ASCs demonstrated enhanced adipogenic differentiation based on both increased PPARγ expression (Fig. 4B) and lipid accumulation (Fig. 4C), as compared to FAP$^{+/+}$ ASCs. Since we had not observed differences of various lineage markers in the starting population (Fig. 3A, S3), it was unlikely that the observed divergence in differentiation was due to different amounts of adipocyte progenitors in FAP$^{+/+}$ and FAP$^{-/-}$ ASC populations. Still, to assess if acute loss of FAP from a single population is sufficient to enhance adipogenesis, we performed acute knockdown of FAP by treating FAP$^{+/+}$ ASCs with shFAP prior to differentiation. Acute loss of FAP was sufficient to enhance both PPARγ expression (Fig. 4D) and lipid accumulation (Fig. 4E), though even small amounts of residual FAP (Fig. 4F) inhibited these effects. Together these data indicate that loss of FAP enhances the adipogenic potential of ASCs, representing a cell-intrinsic mechanism underlying the hyperplasia/hypertrophy phenotype and exaggerated weight gain we observed in FAP$^{-/-}$ mice.

FAP deletion promotes non-fibrillar collagen accumulation

To address potential cell-extrinsic mechanisms of adipocyte hypertrophy, we profiled the ECM and
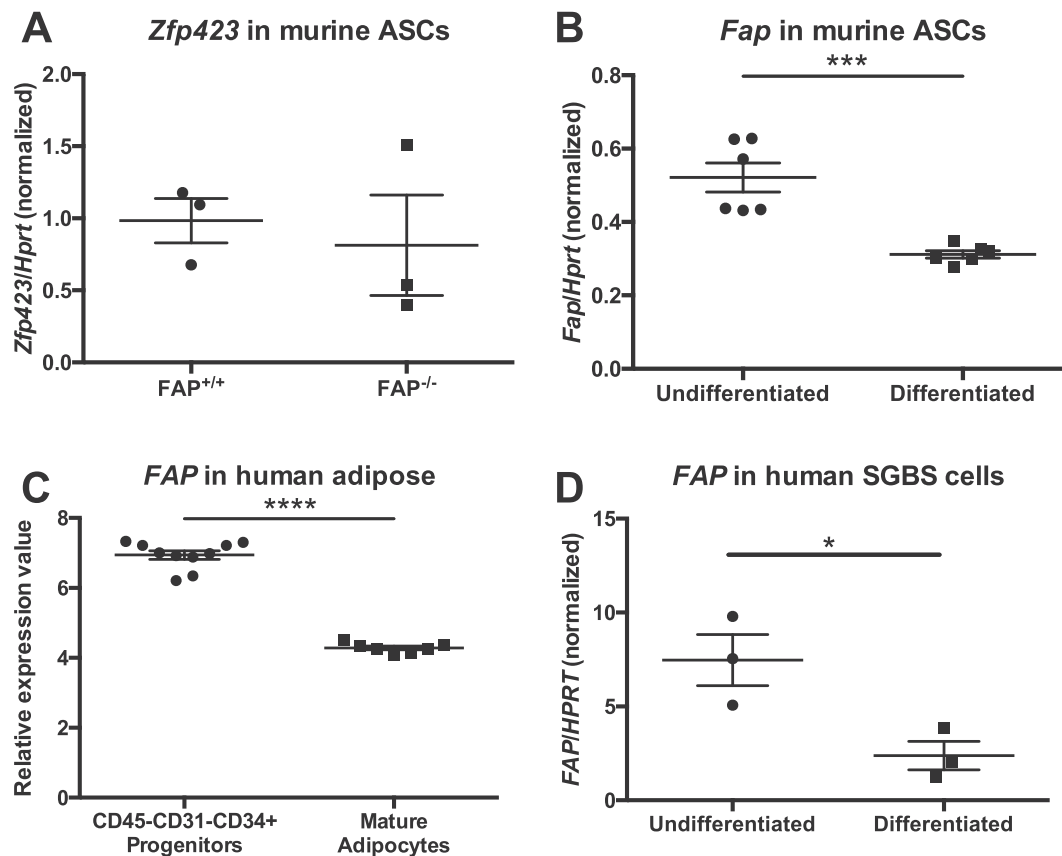
A ***Zfp423* in murine ASCs**

B ***Fap* in murine ASCs**

C ***FAP* in human adipose**

D ***FAP* in human SGBS cells**

Fig. 3. *FAP is down-regulated on mature adipocytes.* A)) qRT-PCR analysis of expression of the preadipocyte marker Zfp423 in freshly isolated murine ASCs (FAP$^{+/+}$ and FAP$^{-/-}$). B) qRT-PCR analysis of FAP expression on primary murine ASCs with and without adipogenic differentiation stimuli. C) Microarray analysis [18] of FAP expression in human adipose progenitors (CD45-CD31-CD34+) and mature (buoyant) adipocytes. D) qRT-PCR analysis of FAP expression on a human pre-adipocyte cell line with and without adipogenic differentiation stimuli. For all of the above: statistical analysis by two-tailed *t*-test. Each point represents cells harvested from an individual mouse/patient.

adhesion receptor expression of isolated FAP$^{+/+}$ and FAP$^{-/-}$ ASCs using a Qiagen RT^2 Profiler PCR array. In the absence of differentiating or activating stimulus, we did not find highly significant changes in any individual genes, but did see an overall shift towards increased expression of various functional groups of factors, including cell-ECM adhesion receptors, cell-cell adhesion receptors, and ECM-modulating proteases (Fig. S4, Table S1). This indicated that FAP$^{-/-}$ ASCs might differentially interact with various matrix components both *in vitro* and *in vivo*. In light of the collagen transcription RNAseq data (Fig. 2C), we compared the collagen matrix in the subcutaneous fat of FAP$^{+/+}$ and FAP$^{-/-}$, LFD and HFD-fed mice. Using an aniline blue stain for total collagen we saw that HFD was sufficient to increase total collagen accumulation in FAP$^{+/+}$ mice, with an increased effect in the HFD-fed FAP$^{-/-}$ mice as compared to LFD-fed mice (Fig. 5A). Yet when we visualized fibrillar collagen specifically, using second harmonic generation

(SHG) microscopy [24], we saw that HFD-fed FAP$^{-/-}$ mice did not show a concomitant increase in fibrillar collagen specifically (Fig. 5B). Using a picrosirius red stain visualized under circular polarized light, we were able to quantify the relative collagen fiber width in subcutaneous fat. Thin fibers appear green in this analysis, intermediate fibers red or pink, and thick, well-formed fibers yellow. We saw a reduction in the amount of yellow, thick fibers selectively in HFD-fed FAP$^{-/-}$ mice (Fig. 5C). Taken together, these data indicate that FAP$^{-/-}$ adipose accumulated more total collagen but exhibited reduced collagen remodeling, specifically fiber accumulation, when challenged with HFD. Since FAP is known to play a role in fibrillar collagen degradation and recycling, this could be due to the accumulation of partially digested collagen fibers [25]. We also performed aniline blue staining and SHG in visceral fat. Overall, visceral fat showed much less collagen, both total and fibrillar. In HFD-fed mice, FAP deletion did not alter total collagen accumulation (Fig. S5A),

but resulted in reduced fibrillar collagen specifically (Fig. S5B), again implicating impaired collagen remodeling.

FAP deletion reduces collagen fibrillogenesis

To investigate these differences in collagen in more detail, and to test whether these alterations in collagen are attributable to ASC-mediated matrix remodeling, we generated cell-derived matrices (CDMs) *in vitro* using primary ASCs isolated from the subcutaneous fat of FAP$^{+/+}$ and FAP$^{-/-}$ mice

(Fig. 6A), where we had seen the most marked collagen accumulation. These matrices recapitulated the differences observed *in vivo* between FAP$^{+/+}$ and FAP$^{-/-}$ adipose ECM in the context of HFD. Specifically, more overall collagen accumulated in FAP$^{-/-}$ CDMs, as measured by a colorimetric assay for picrosirius red dye binding (Fig. 6B, S6A), but this increase in total collagen was not associated with an increase in total fibrillar collagen as measured by SHG signal (Fig. 6C, S6B), or with any difference in overall stiffness as measured by atomic force microscopy (Fig. S6C). In line with
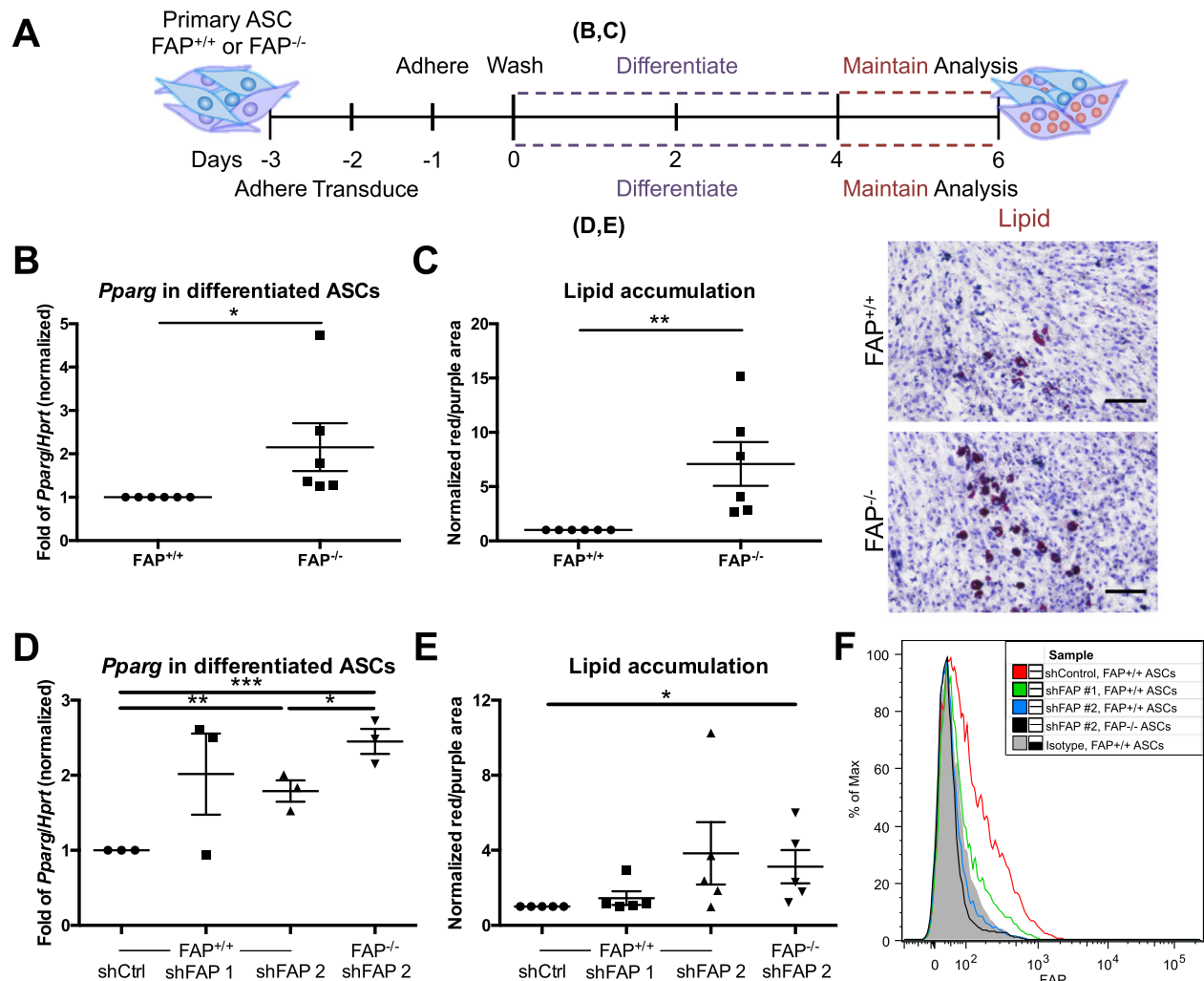

Fig. 4. *FAP restricts adipogenesis.* A) Experimental schematic of *in vitro* differentiation. B) qRT-PCR analysis of PPARγ expression in differentiated murine ASCs (FAP$^{+/+}$ and FAP$^{-/-}$). C) ORO stain for lipid accumulation in differentiated ASCs (scale bar $=100\,\mu m$). D) qRT-PCR analysis of PPARγ expression in differentiated murine ASCs following acute knockdown of FAP *via* lentiviral shRNA. E) ORO stain for lipid accumulation in ASCs differentiated following shRNA treatment. For all of the above: statistical analysis by two-tailed ratio paired *t*-test on raw values. Each point represents cells harvested from an individual mouse F) Flow cytometry for surface FAP expression 48 h post-transduction with lentiviral shRNA. One representative graph of three independent experiments.
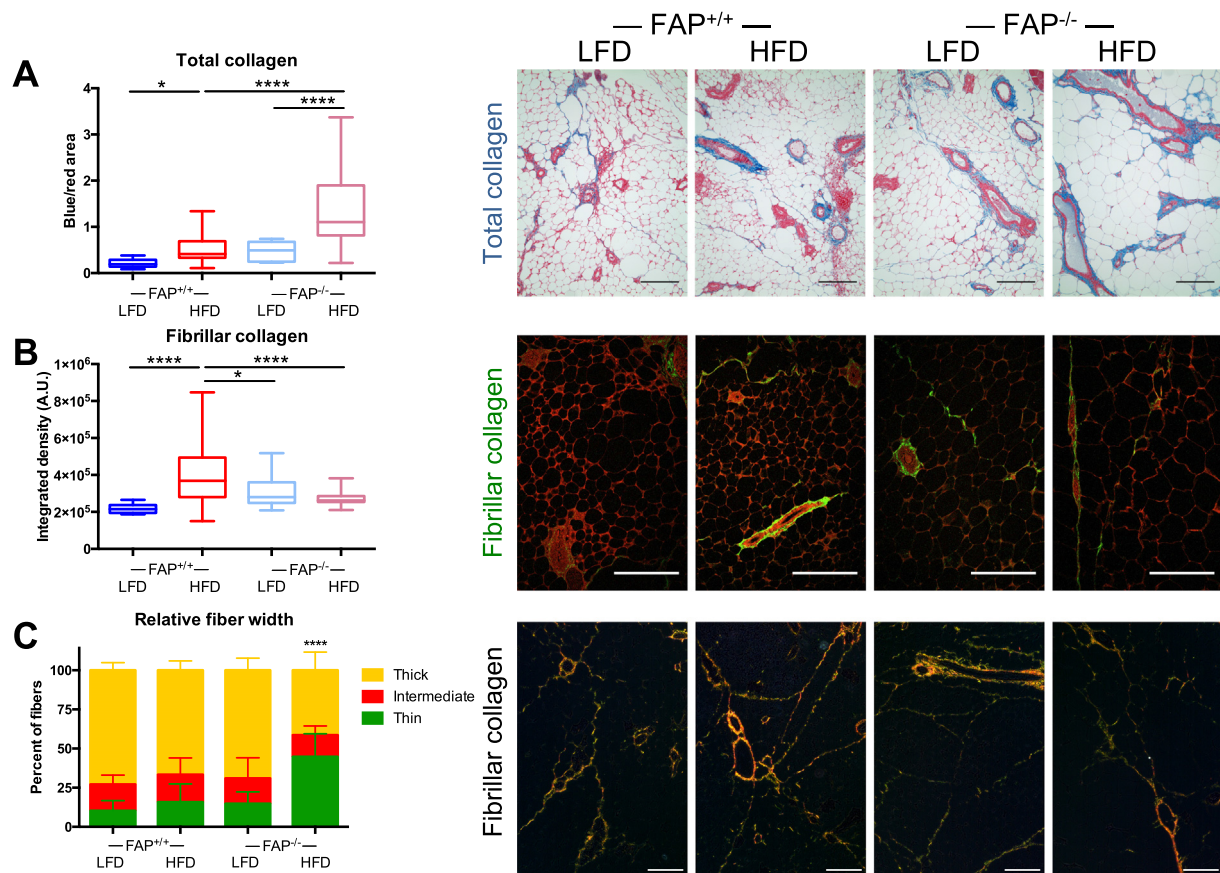
Fig. 5. *FAP deletion promotes accumulation of collagen in non-fibrillar forms.* A) Total collagen measured by aniline blue in subcutaneous fat (N = 3−7 mice/group, 3 images/mouse). Scale bars = 200 μm; statistical analysis by two-way ANOVA. B) Fibrillar collagen measured by SHG in subcutaneous fat (N = 3−7 mice/group, 5 images/mouse). Scale bars = 200 μm; statistical analysis by two-way ANOVA. C) Fibrillar collagen imaged by picrosirius red stain under circular polarized light, where thin fibers appear green, intermediate fibers red, and thick fibers yellow (N = 3−7 mice/group, 5 images/mouse). Scale bars = 200 μm; statistical analysis by chi-square test.

these data, we saw no difference in the expression of the fibrillar collagens I and III as quantified by qPCR (Fig. 6D, E). However, expression of collagen XI was selectively reduced (Fig. 6F) in FAP$^{−/−}$ CDMs, as it also was in our RNAseq analysis (Fig. 2C). Collagen XI is a minor fibrillar collagen that plays a role in nucleating fibrillogenesis [26], consistent with the possibility that this selective reduction in collagen XI expression may have contributed to the impaired collagen fiber formation associated with FAP deletion. In addition, we found that levels of lysyl oxidase (LOX) were also markedly reduced in FAP$^{−/−}$ cells compared to FAP$^{+/+}$ (Fig. 3H). Hydroxylation of collagen chains by LOX underpins their ability for form fibers, so this reduction provides additional evidence for mechanisms by which FAP deletion led to impaired collagen fibrillogenesis. The increased total collagen, meanwhile, might have been due to increased expression or impaired degradation of still other collagen types. This is, as far as we are aware, the first direct evidence that FAP or FAP-dependent

matrix remodeling creates an autocrine feedback loop to regulate production and post-translational modifications of fibrillar collagens.

FAP$^{−/−}$ ASC-derived matrix is sufficient to promote adipocyte lipid accumulation

Since we were able to model the observed *in vivo* matrix differences caused by FAP deletion using the CDM approach *in vitro*, we used this same approach to test whether the distinct matrix produced by FAP$^{−/−}$ ASCs might be sufficient to directly enhance adipocyte hypertrophy. We again used primary ASCs from FAP$^{+/+}$ and FAP$^{−/−}$ mice to generate CDMs. The CDMs were decellularized by detergent lysis, leaving the intact matrix free of ASCs. In these experiments we employed the 5A pre-adipocyte cell line [27], which provided a more homogenous starting population than primary ASCs. We plated these immortalized pre-adipocytes onto FAP$^{+/+}$ or FAP$^{−/−}$ CDMs and induced differentiation using the
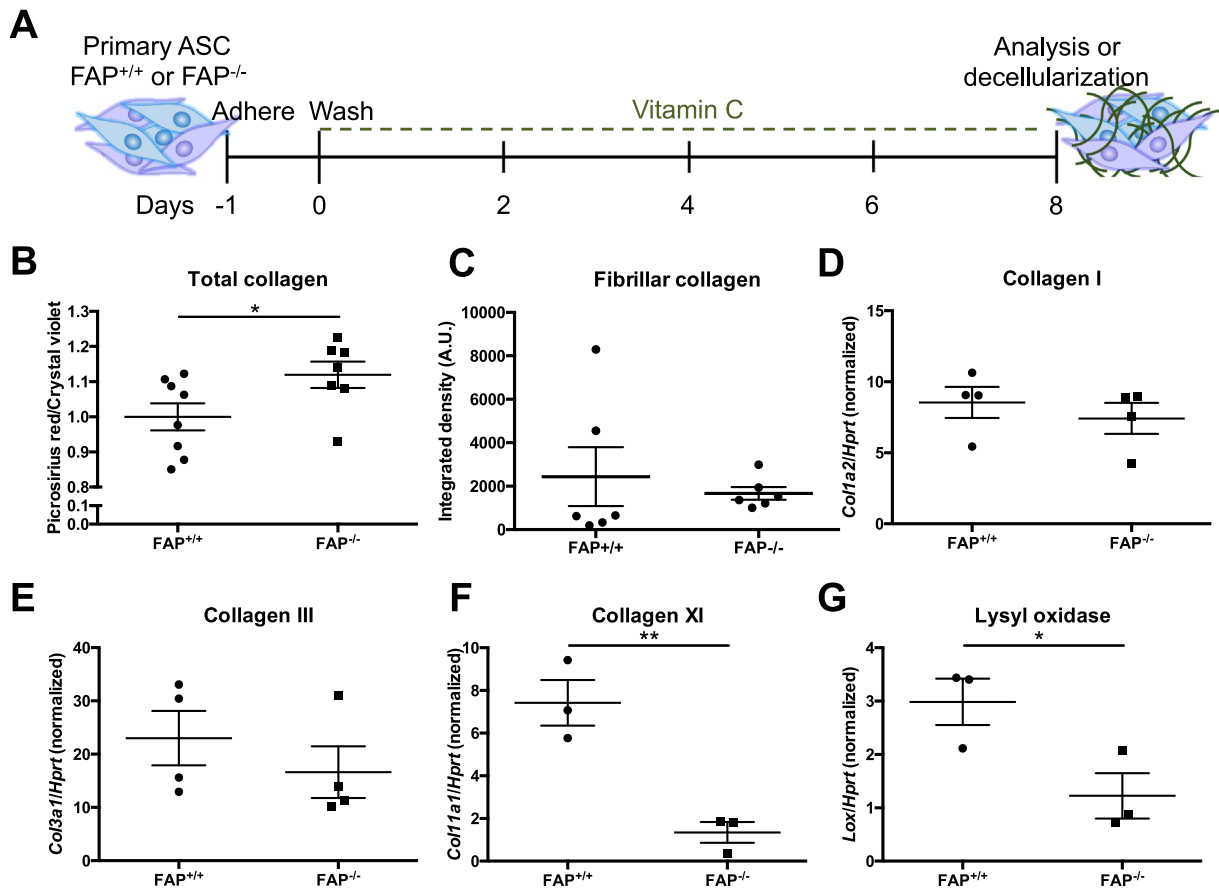
Fig. 6. *FAP deletion reduces collagen fibrillogenesis.* A) Experimental schematic for CDM generation B) Total collagen in CDMs measured by picrosirius red dye binding colorimetric assay. C) Fibrillar collagen in CDMs measured by SHG D) qRT-PCR analysis of Collagen I, E) Collagen III, F) Collagen XI, and G) Lysyl oxidase expression in CDM-laying ASCs. For all of the above: statistical analysis by two-tailed t-test. Each point represents cells harvested from an individual mouse.

same protocol described above (Fig. 7A). Similar to the ASC differentiation and human data, pre-adipocytes showed dramatic loss of FAP expression as they underwent *in vitro* differentiation (Fig. 7B). Although we observed no differences in PPARγ expression in 5A cells post-differentiation on matrix derived from $FAP^{+/+}$ and $FAP^{-/-}$ ASC (Fig. 7C), there was a marked difference in lipid accumulation as measured by ORO staining (Fig. 7D). These results suggest that the alterations in matrix had little effect on adipogenic differentiation at a transcriptional level, but that matrix can modulate adipocyte lipid metabolism and thereby hypertrophy. We next tested whether this difference in lipid accumulation was due predominantly to uptake of exogenous lipid or to *de novo* lipid synthesis. We differentiated pre-adipocytes on $FAP^{+/+}$ or $FAP^{-/-}$ matrix for four days, and then switched to maintenance in media containing either FCS or delipidated FCS for an additional four days. In the absence of exogenous lipid, the difference in lipid accumulation was partially

ablated (Fig. 7E), suggesting that matrix affected both uptake and production of lipid by adipocytes.

$FAP^{-/-}$ ASC-derived matrix promotes FAK/ mTOR signaling

We hypothesized that one mechanism that might underlie the phenotype described above was mTOR signaling, which is known to lie upstream of lipid synthesis [28] and was one of the differentially regulated gene networks revealed by our RNAseq experiment (Fig. 2B). In order to test this hypothesis, we inhibited mTOR in pre-adipocytes starting on the fourth day of differentiation, using rapamycin (Fig. 8A). After 8 h, we assessed mTOR activity by S6 kinase[Thr389] phosphorylation, and found that mTOR activity was higher at baseline in cells cultured on $FAP^{-/-}$ matrix, and dramatically reduced in either condition by Rapamycin (Fig. 8B). We also assessed expression levels of various mTOR target genes that are directly involved in lipid synthesis, and discovered
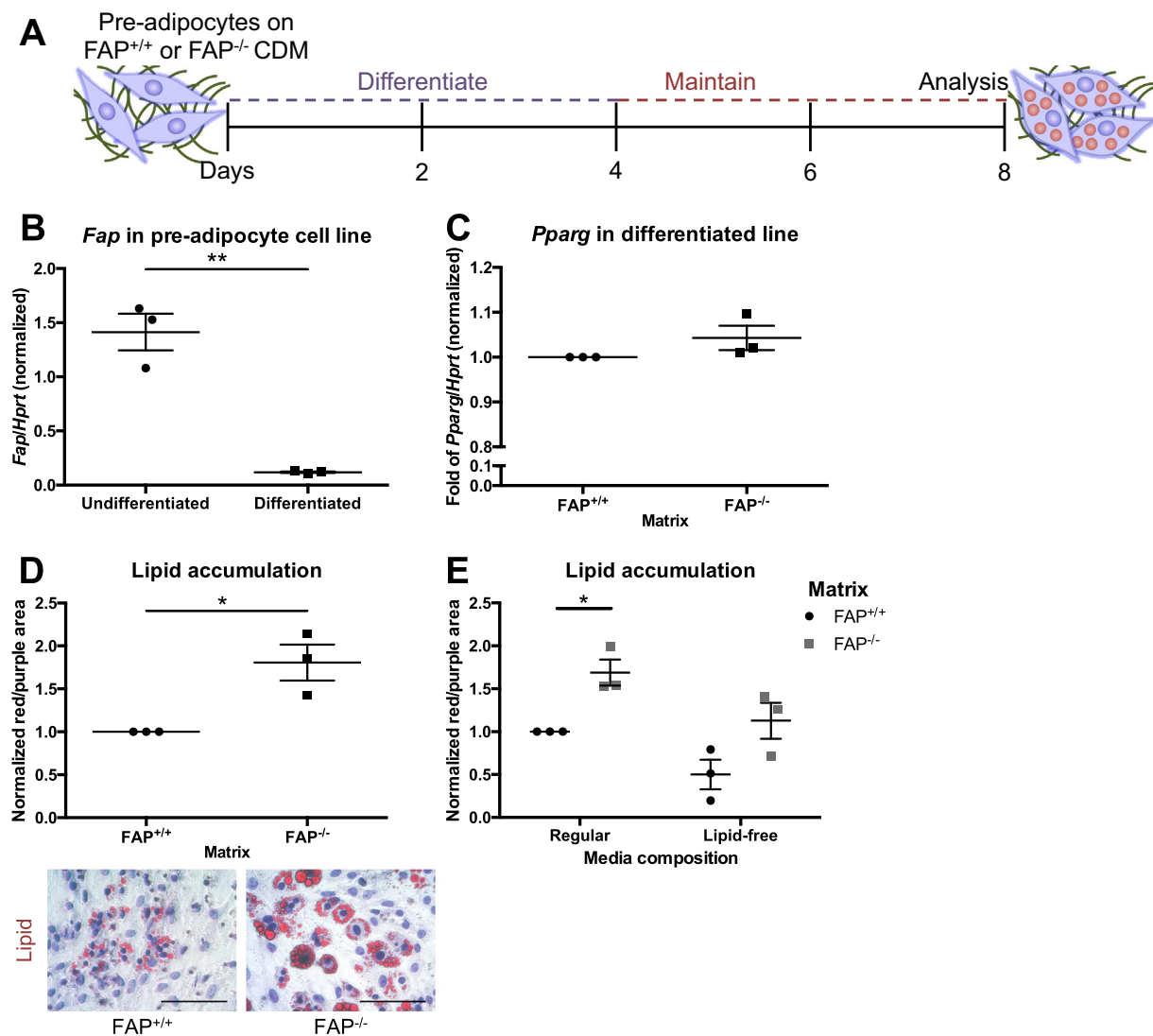
Fig. 7. *Matrix laid by FAP$^{-/-}$ ASCs enhances lipid accumulation of pre-adipocytes.* A) Experimental design for testing the effects of matrix on pre-adipocyte lipid accumulation. B) qRT-PCR analysis of FAP expression on pre-adipocytes with and without differentiation. C) qRT-PCR analysis of PPARγ expression following differentiation of pre-adipocytes on FAP$^{+/+}$ and FAP$^{-/-}$ CDMs. D) ORO stain for lipid accumulation in pre-adipocytes following differentiation on FAP$^{+/+}$ and FAP$^{-/-}$ CDMs (scale bars =100 μm). E) ORO stain for lipid accumulation in pre-adipocytes in the presence or absence of exogenous lipid, on FAP$^{+/+}$ and FAP$^{-/-}$ CDMs. For all of the above: statistical analysis by two-tailed ratio paired t-test. Each point represents CDMs generated from an individual mouse.

that culture on FAP$^{-/-}$ matrix is sufficient to enhance their expression relative to culture on FAP$^{+/+}$ matrix (Fig. 8E), supporting a role for FAP$^{-/-}$ matrix-induced mTOR signaling in *de novo* lipid synthesis of differentiating adipocytes. One possible link between FAP$^{-/-}$ matrix and mTOR signaling is FAK, which lies downstream of integrin signaling and upstream of mTOR *via* PI3K and AKT. We inhibited FAK starting on day four of differentiation using the small molecule inhibitor PF573228 (Fig. 8A). While we did not note overt differences in FAK^{Tyr397} phosphorylation between cells on FAP$^{+/+}$ or FAP$^{-/-}$ matrix

(Fig. 8C), we did observe that FAK inhibition selectively reduced S6 kinase phosphorylation in the cells on FAP$^{-/-}$ matrix (Fig. 8D). This indicates that, while levels of FAK activation were not different on FAP$^{+/+}$ and FAP$^{-/-}$ matrix, the signaling pathways downstream of FAK were different depending on matrix and that cells grown on FAP$^{-/-}$ matrix seemed uniquely reliant on FAK-activated mTOR signaling. Ultimately, and in agreement with this conclusion, inhibition of FAK selectively reduced the lipid accumulation phenotype in cells cultured on FAP$^{-/-}$ matrix, ablating the matrix-induced
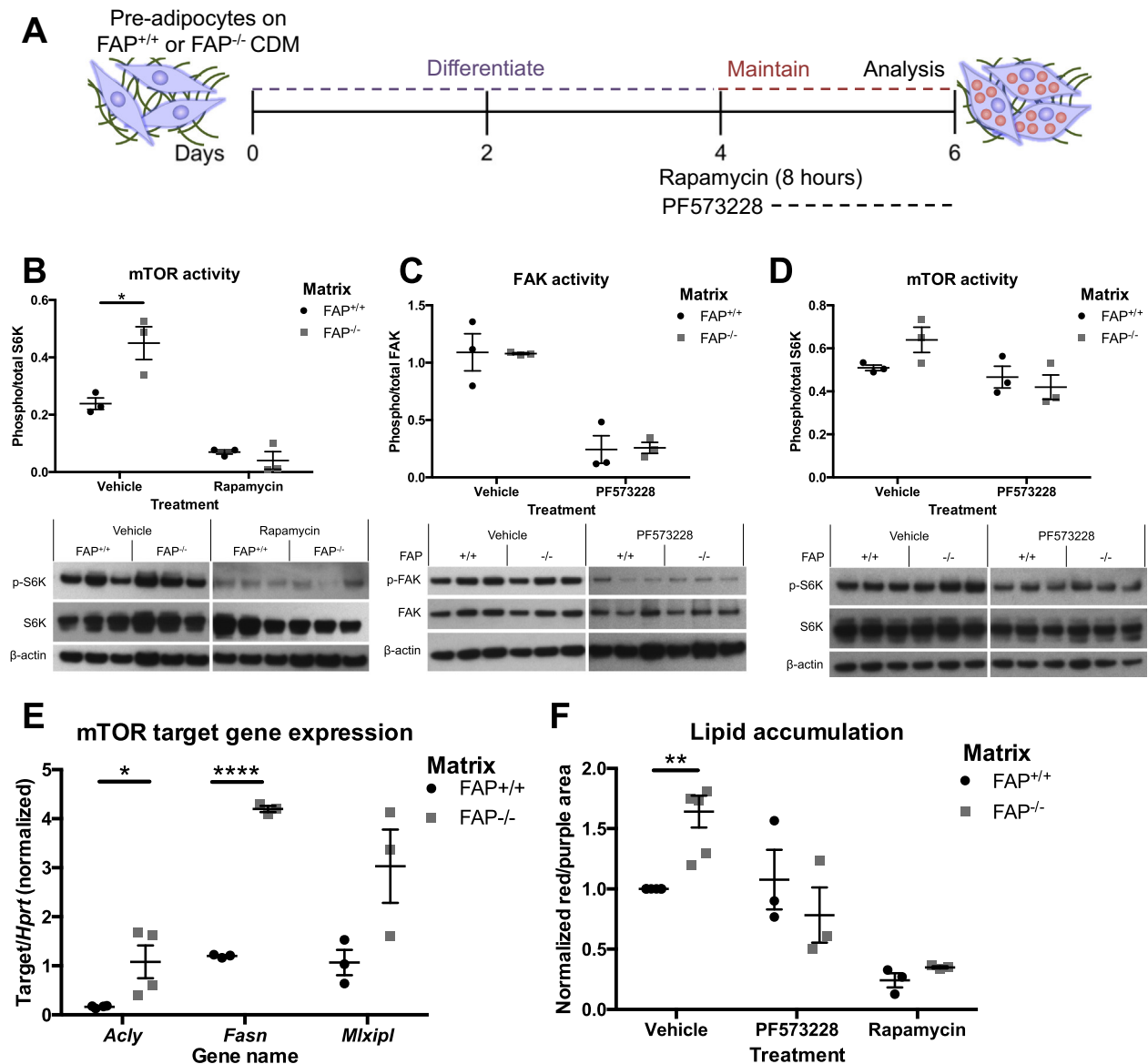
Fig. 8. *Matrix laid by FAP$^{-/-}$ ASCs enhances lipid accumulation of pre-adipocytes via FAK and mTOR pathways*. A) Timeline for various inhibitor treatments during pre-adipocyte differentiation. B) Immunoblot for phospho- *vs.* total S6K in pre-adipocytes on day four of differentiation on FAP$^{+/+}$ and FAP$^{-/-}$ CDMs, with and without 8 h Rapamycin treatment. C) Immunoblot for phospho- *vs.* total FAK and D) S6K in on day six of differentiation on FAP$^{+/+}$ and FAP$^{-/-}$ CDMs, with and without FAK inhibition for two days. For all blots, density of total and phospho bands was first normalized to β-actin loading control before calculating phospho/total ratio. Statistical analysis by two-tailed ratio paired t-test. E) qPCR analysis of mTOR targets ACLY, FAS, and ChREBPβ in pre-adipocytes differentiated on FAP$^{+/+}$ and FAP$^{-/-}$ CDMs. Statistical analysis by two-tailed t-test. F) ORO stain for lipid accumulation on day six of differentiation on FAP$^{+/+}$ and FAP$^{-/-}$ CDMs, with FAK or mTOR inhibition compared to vehicle control. Statistical analysis by two-tailed ratio paired t-test. Each point represents CDMs generated from an individual mouse.

difference in lipid accumulation (Fig. 8F). Inhibition of mTOR significantly reduced lipid accumulation in all cells, and also ablated the differences observed between cells on FAP$^{+/+}$ or FAP$^{-/-}$ matrix (Fig. 8F). This indicates that FAP$^{-/-}$ matrix enhances mTOR signaling *via* FAK, and that these signaling pathways lead to the enhanced lipid accumulation observed on FAP$^{-/-}$ CDMs.

Discussion

In this study, we demonstrated a novel role for fibroblast activation protein in regulating weight gain and adipocyte hypertrophy. In particular, we discovered that FAP expression by pre-adipocytes provides a cell-intrinsic restriction on adipogenic differentiation, but also that FAP-mediated collagen

remodeling alters lipid metabolism in mature adipocytes. We also demonstrate that loss of FAP—which is known as a collagen-degrading enzyme—impairs collagen fiber accumulation, suggesting a novel link between matrix degradation and fibrillogenesis. All together, in an intact organism, loss of FAP results in accumulation of non-fibrillar collagen in white adipose tissue, increased adipocyte hypertrophy, and enhanced overall weight gain (working model, Fig. S7).

Collagen-rich ECM plays a central role in regulating cell and tissue biology in diverse organs and disease states. In this study, we demonstrated a link between FAP-associated collagen remodeling and obesity. In particular, we provided evidence for a FAK-mediated link between matrix and the mTOR signaling pathway, which promotes lipid accumulation in adipocytes [28]. These results suggest that obesity-related adipose fibrosis is a key player in the disease and not merely a hallmark, and also highlights the need to account for matrix in cellular models even of well-established pathways like mTOR. Ultimately, our study contributes to the emerging understanding that it is the quality of the ECM, and not merely the extent of fibrosis as measured by collagen content, that is relevant to promoting or restraining disease [13,15].

In terms of the effects of loss of FAP on ECM quality, we have provided evidence that various stages of collagen metabolism are coupled. In particular, loss of FAP also results in reduced fibrillogenesis, associated with reduction in collagen XI and lysyl oxidase, all of which may possibly be due to biochemical feedback from partially digested collagen fragments. A recent study demonstrated physical and functional interactions between members of the LOX and ADAMTS families [29], data which are interesting in light of our discovery of both changes in LOX expression during CDM deposition and alterations to baseline ADAMTS protein expression in $FAP^{-/-}$ ASCs. Future studies could follow these observations and investigate roles for FAP in this molecular interaction. In additional future studies, it would be valuable to identify which ECM-receptors are engaged by $FAP^{-/-}$ matrix and activate the FAK/mTOR signaling we observed. Interestingly, prior studies have shown that pre-adipocytes express the collagen-binding integrin subunits $\alpha2$ and $\alpha11$, while mature adipocytes upregulated $\alpha1$ and $\alpha10$ [30]. Intriguingly, subunits $\alpha2$ and $\alpha11$ have been reported to strongly bind fibrillar collagen, while $\alpha1$ and $\alpha10$ have increased avidity for collagen in non-fibrillar configuration [31]. This could suggest that $FAP^{-/-}$ matrix, which contains reduced fibrillar collagen, is better suited to engage the integrins that mature adipocytes naturally express.

Questions also remain as to the exact mechanisms underlying our observation that FAP is able to restrict adipogenic differentiation. In other contexts, FAP has been observed to act through both enzymatic and non-enzymatic means [17], so the most pressing question is if FAP's protease activity is required to restrain differentiation. If this phenomenon is indeed due to FAP's enzymatic activity, it may be that collagen cleavage releases signaling moieties from the ECM that then can act on preadipocytes, either locally or distally, to regulate differentiation of progenitors to mature adipocytes. This would be analogous to the role played by endotrophin, a collagen VI cleavage product that promotes fibrosis and inflammation in obese adipose [32]. It is also possible, however, that the mechanism relies on FAP's association with various other molecules in the plasma membrane, where it may bring together signaling complexes that can have downstream effects on transcriptional profiles [33]. Indeed, Thy-1 (CD90), which associates with FAP in lipid rafts, has also been reported to restrain adipogenesis by preferentially supporting osteogenesis in mesenchymal stem cells [34]. Future studies will be needed to address which of these mechanisms is most relevant.

While our *in vitro* experiments with isolated ASCs provide evidence for two mesenchymal-cell mediated mechanisms underlying this obesity phenotype, our mouse model is a global FAP knockout and so we must consider the possible involvement of other cell types involved in weight gain. FAP expression is typically restricted to mesenchymal cells, but in the context of cancer has been noted on a subset of M2-like macrophages [35]. Macrophages and systemic inflammation do play a critical role in the pathogenesis of obesity, and so it is entirely possible that FAP deletion also results in alterations to macrophage function which in turn change the response to high-fat diet. This hypothesis will be pursued in additional studies. Another remaining area of study surrounding FAP and obesity is the effects of FAP deletion on the metabolism and function of its substrates other than collagen. Of particular interest to human obesity is FGF21, which is upregulated in obesity and regulates glucose and lipid homeostasis [36]. FAP is able to cleave and inactivate FGF21, thus presumably exacerbating obesity-associated metabolic dysfunction [37]. Loss or inhibition of FAP, therefore, would allow for normal FGF21 function and improved metabolism. While this interaction would be extremely relevant to our studies, murine FGF21 is resistant to FAP cleavage, and thus our mouse model is not useful for studying this fascinating interaction [38].

Based on an earlier report that treatment of mice with the FAP and DPP inhibitor talabostat may improve glucose metabolism [39], another recent study examined the role of FAP in systemic glucose regulation [40]. Specifically, weight gain and glucose metabolism were compared in male C57BL/6 J $FAP^{+/+}$ and $FAP^{-/-}$ mice, with and without the

FAP inhibitor CPD60, while in our study $FAP^{+/+}$ and $FAP^{-/-}$ female FVB mice were analyzed. We observed enhanced weight gain without impaired glucose response in the absence of any differences in food intake in the $FAP^{-/-}$ mice compared to $FAP^{+/+}$ mice. In the former study, male C57Bl/6 mice that were $FAP^{-/-}$ or treated with FAP inhibitor showed reduced food intake, which may explain why they did not display enhanced weight gain, but did show improved glucose metabolism. Therefore, the results in these two studies do not contradict each other, but rather, the phenotypic differences noted more likely reflect either the fact that food intake was altered in one case not the other, and/or differences in strain and sex. In fact, the conclusion of both studies is that FAP has minimal effects on systemic metabolism [40], This led us to investigate much more closely the local adipose microenvironment. Indeed, local biomarkers have been reported to correlate even more strongly to metabolic heath than global metrics like BMI; in particular, the presence of crown structures, or macrophage-containing inflammatory foci [41]. Here we present a mesenchymal fibrotic response as also potentially serving as a hallmark for metabolic health. Indeed, prior studies have suggested that individuals with impaired adipogenesis may be more likely to display unfavorable metabolic profiles and insulin resistance [42,43]. The role for FAP in restraining adipogenic differentiation we have found here might contribute to a similar metabolic dysfunction, while $FAP^{-/-}$ mice, able to undergo adipose expansion *via* enhanced adipogenic differentiation, could be more metabolically stable. On a cellular level, less rigid ECM has been hypothesized to alleviate biomechanical stress on adipocytes, thus resulting in what might be called 'metabolically healthy' hypertrophy [13]. In the future, it would also be valuable to elucidate the effects of FAP knockout on various biomechanical properties of adipose tissue.

FAP has not been widely studied in terms of human genetic variation. In the European Bioinformatics Institute genome-wide association study catalog, genetic variants in the intergenic region between FAP and IFIH1 have been associated with total cholesterol [44] and type 1 diabetes risk [45], but these studies did not investigate potential contributions of FAP. Nevertheless, the novel roles we have described for FAP in restraining adipogenic differentiation, mediating collagen fibrillogenesis, and stimulating mTOR signaling in adipocytes could all have profound effects on the incidence of various diseases, like cancer, which are often observed secondary to obesity. As with our observations on fibrosis, this highlights that, in terms of disease risk and severity, mere amount of weight gain (*e.g.* body mass index) is less important than understanding the cellular and molecular qualities of adipose tissue. In particular, identifying situations where higher body mass does not result in worse pathology may provide crucial windows of therapy for various diseases, including cancer, diabetes, and cardiovascular disease.

Materials and methods

Animal studies

$FAP^{-/-}$ mice with luciferase knock-in at both FAP alleles were backcrossed to FVB mice (Jackson Labs) for at least 8 generations. Female FVB mice (bred in house as $FAP^{+/+}$ or $FAP^{-/-}$) were fed special diet *ad libitum* from 12 weeks of age to 30 weeks of age. Special diets were D12492i (60 kcal% fat) and D12450Bi (10 kcal% fat) from Research Diets Inc. (New Brunswick, NJ). Cages of 2−5 mice were randomly assigned to high-or low-fat diet. All mouse breeding and experimental procedures were conducted in accordance with protocols approved by the University of Pennsylvania Institutional Animal Care and Use Committee.

RNAseq

30-week-old female FVB mice ($FAP^{+/+}$ and $FAP^{-/-}$) were euthanized by CO_2 inhalation. Total subcutaneous mammary fat was harvested and 100−180 mg frozen tissue per mouse was flash frozen and then homogenized in 1.4 ml Qiazol lysis buffer with an Omni-TH tissue homogenizer before being passed 6 times through a 20-G needle. RNA was extracted according to the manufacturer's protocol for Qiagen RNeasy kits. RNA quality was assessed *via* bioanalyzer and then sequencing libraries generated using Illumina TruSeq Stranded Total RNA LT kit. Read mapping as carried out using kallisto and subsequent analysis carried out in R studio. RNAseq data is deposited at NCBI Gene Expression Omnibus (accession number GSE119633).

Primary cell isolation and culture

Primary adipose stromal cells (ASCs) were harvested from female FVB mice ($FAP^{+/+}$ and $FAP^{-/-}$) after euthanasia by CO_2 inhalation at 8−12 weeks of age. Total subcutaneous mammary fat was diced and placed in a 10 ml cocktail of 250 μg/ml each of collagenases 1, 2, and 4 (Worthington CLS-1 and CLS-2; Sigma-Aldrich C9891). Tissues were digested for 90 min at 37 °C on a rocker. Single cell suspensions were recovered by filtration of digested tissue through a 70-μm strainer with equal volume 10% FCS/DMEM, pelleted by centrifugation, and resuspended in complete media (DMEM with 10% FCS, 1 mM L-glutamine, 10 U/ml penicillin-streptomycin, 0.25 μg/ml amphotericin B, 50 μg/ml

gentamicin) before being plated in 10 cm tissue culture plastic dishes. Cells were incubated at 37 °C overnight and then washed 3× with PBS to remove non-adherent cells.

Murine pre-adipocyte culture

Immortalized murine pre-adipocyte cell lines generated as previously described [22] were generously provided by Dr. Kathryn Wellen (U. Penn.) and cultured in DMEM/F12 with 10% FCS, 1 mM L-glutamine, 10 U/ml penicillin- streptomycin.

In vitro murine adipocyte differentiation

Primary ASCs (passage 1) or immortalized pre-adipocytes (passage 12−17) were seeded at confluency in either 12- or 6-well plates (4×10^4 and 1×10^5 cells/well, respectively). Cells were cultured in complete media with 1.5 µg/ml insulin (Sigma-Aldrich I0516), 0.5 mM IBMX (Sigma-Aldrich I5879), and 0.5 uM dexamethasone (Sigma-Aldrich D4902) for four days and then for an additional 2−4 days in complete media with 1.5 µg/ml insulin alone (media changed every 2 days). Where applicable, complete media made with delipidized FCS (Gemini Bio-Products 900−123) was applied, with insulin, for the final four days of differentiation. Differentiation was then assessed by qRT-PCR for PPARγ and Oil-red-O staining. Where applicable, 20 nM PF573228, 2 nM rapamycin, or DMSO alone were added to maintenance media at day 4.

Human pre-adipocyte culture and differentiation

SGBS cells were cultured and differentiated as previously described [37,38]. Briefly, standard culture occurred in DMEM/F12 with 10% FCS, 100 U/ml penicillin-streptomycin, 3.3 mM biotin, and 1.7 mM panthotenat. Differentiation was induced for 4 days with added transferrin, insulin, cortisol, triiodothyronine, dexamethasone, IBMX, and rosiglitazone. Cells were maintained in base media with added transferrin, insulin, cortisol, and triiodothyronine for an additional 10 days before RNA extraction and qPCR analysis.

FAP knockdown *via* shRNA

FAP-targeting MISSION® shRNA constructs were purchased as bacterial glycerol stocks (Sigma-Aldrich SHCLNG-NM_007986), while non-targeting control was purchased as plasmid (Sigma-Aldrich SHC016-1EA) and introduced to competent cells. The construct labeled shFAP #1 is Sigma-Aldrich TRCN0000031326 and #2 is TRCN0000031324. Plasmid DNA was purified using Qiagen Plasmid Maxi Kits (Cat. No 12162) according to the manufacturers protocol. Lentiviral vectors were produced by triple-transfection of sh-plasmids (9 µg/ml) with

pCMVΔR2.8 (9 µg/ml) and pMD2.G (3 µg/ml) packaging vectors into HEK293T cells. Resulting viral supernatant was titered using a p24 ELISA-based kit (Cell Biolabs, Inc. VPK-107). Primary ASCs were treated with MOI 10 viral particles and 8 µg/ml polybrene overnight. 48 h after initial exposure to viral particles, cells were either assessed for FAP expression *via* flow cytometry, or began adipogenic differentiation as above.

Flow cytometry

ASCs were harvested, resuspended in 2% FCS/PBS at 5×10^5 cells/200 µl, and transferred to a v-bottom 96 well plate. They were incubated 15 min with an Fc receptor blocking antibody (eBioscience 14−0161), 30 min with a biotinylated anti-FAP antibody (clone 73.3 available from EMD Millipore), and 15 min with streptavidin-conjugated brilliant violet 421 (Biolegend 405,225), with two washes in between each incubation. Stained cells were finally resuspended in 2% FCS/PBS with propidium iodide and immediately run on a BD LSRFortessa cytometer.

qRT-PCR

RNA was extracted according to the manufacturer's protocol for TRIzol (Life Technologies 15596) and then converted to cDNA using a high-capacity reverse transcription kit (ThermoFisher 4368814). PCR was performed using SYBR Green reagents (ThermoFisher 4309155)

Oil-red-O stain

Cells were fixed in 4% PFA, equilibrated in 60% isopropanol, and then reacted with Oil-red-O (Sigma Aldrich O1391) for 10 min. Cells were then washed until rinsed clear, counterstained with hematoxylin (Thermo Scientific 7231) for 1 min, and then washed again.

RT^2 profiler PCR array

Primary ASCs were isolated from three each FAP$^{+/+}$ and FAP$^{-/-}$ mice as above (Methods 4.3) and cultured for three days to expand. Cells were trypsinized, counted, and then 3×10^6 cells were lysed in Qiagen RLT buffer for RNA extraction using the RNeasy mini kit. cDNA first strand synthesis was performed using the RT^2 first strand kit and the qPCR array carried out according to the manufacturer's protocol (Qiagen PAMM-013Z). Analysis was performed in the GeneGlobe Data Analysis Center.

Cell-derived matrices (CDMs)

As described previously (Beacham, 2001), 12- or 6-well plates were coated with cross-linked gelatin

(0.2%), and then p2 primary ASCs plated at 2×10^5 cells/well in 12-well plates or 5×10^5 cells/well in 6-well plates. Cells were allowed to adhere overnight, and then treated with 75 µg/ml vitamin C in fresh media every other day for 8 days. For deceullarization, matrices were treated with 0.5% TritonX-100 and 20 mM NH_4OH (in PBS).

Protein lysate preparation

Cell lysis buffer (150 mM NaCl, 50 mM Tris, 1% TritonX-100) was supplemented with 5 mM sodium fluoride, 1 mM sodium orthovanadate, and $1\times$ protease inhibitor cocktail (Roche 11697498001). Complete lysis buffer was added to adherent cells on ice (100 µl/well of 12-well plate) for 5 min before lysate was scraped into eppendorf tubes. Lysates were vortexed briefly, aliquotted, and stored at $-20\,^{\circ}$C. Total protein concentration was determined by Peirce BCA assay.

Immunoblotting

Cell lysates were resolved on $4-12$% Bis-tris NuPage precast gels, and transferred to PVDF membrane *via* a semi-dry transfer. Membranes were blocked in 3% BSA/Tris-buffered saline with 1% Tween (TBST) for 1 h before overnight incubation in primary rabbit antibody at 4 °C (all antibodies from Cell Signaling Technology: S6K, #2708; phospho-S6K^{Thr389}, #9234; FAK, #3285; phospho-FAK^{Tyr397}, #3283; beta-actin, #4967). Membranes were then washed three times with TBST before one hour incubation in HRP-goat anti-rabbit secondary (Sigma Aldrich A0545), and then developed using SuperSignal reagents (Thermo Scientific 34,095). Densitometry quantification was performed in Fiji (ImageJ). Phospho- and total protein bands were normalized to beta-actin loading controls and then data presented as phospho$-$/total ratios.

Statistics

Statistical analysis for all experiments with four groups used 2-way ANOVA with Tukey's multiple comparison tests. Statistical analysis for experiments with two groups used a two-tailed *t*-test on at least three independent replicates.

Data availability

RNAseq data is deposited at NCBI Gene Expression Omnibus (accession number GSE119633).
Supplementary data to this article can be found online at https://doi.org/10.1016/j.matbio.2019.07.007.

Author contributions

R.B. designed and performed experiments, interpreted results, and wrote the paper. D.B. assisted with designing, carrying out, and analyzing the RNAseq experiments. M.W. provided critical material. E.P. designed experiments, contributed to the interpretation of the data, secured funding, and revised the paper.

References

[1] C.M. Hales, M.D. Carroll, C.D. Fryar, et al., Prevalence of obesity among adults and youth: United States, NCHS Data Brief 2017 (2015-2016) 1−8.

[2] D.W. Haslam, W.P.T. James, Obesity, Lancet 366 (2005) 1197−1209.

[3] C. a Gilbert, J.M. Slingerland, Cytokines, obesity, and cancer: new insights on mechanisms linking obesity to cancer risk and progression, Annu. Rev. Med. 64 (2013) 45−57.

[4] A. Divoux, J. Tordjman, D. Lacasa, et al., Fibrosis in human adipose tissue: composition, distribution, and link with lipid metabolism and fat mass loss, Diabetes 59 (2010) 2817−2825.

[5] D. Lin, T.-H. Chun, L. Kang, Adipose extracellular matrix remodelling in obesity and insulin resistance, Biochem. Pharmacol. 119 (2016) 8−16.

[6] T.H. Chun, M. Inoue, H. Morisaki, et al., Genetic link between obesity and MMP14-dependent adipogenic collagen turnover, Diabetes 59 (2010) 2484−2494.

[7] B. Meissburger, L. Stachorski, E. Röder, et al., Tissue inhibitor of matrix metalloproteinase 1 (TIMP1) controls

adipogenesis in obesity in mice and in humans, Diabetologia 54 (2011) 1468−1479.

[8] M. Miana, M. Galán, E. Martínez-Martínez, et al., The lysyl oxidase inhibitor β-aminopropionitrile reduces body weight gain and improves the metabolic profile in diet-induced obesity in rats, Dis. Model. Mech. 8 (2015) 543−551.

[9] Y. Wu, M.-J. Lee, Y. Ido, et al., High-fat diet-induced obesity regulates MMP3 to modulate depot- and sex-dependent adipose expansion in C57BL/6J mice, Am J Physiol Metab 312 (2017) E58−E71.

[10] Y. Zhu, I.L. Kruglikov, Y. Akgul, et al., Hyaluronan in adipogenesis, adipose tissue physiology and systemic metabolism, Matrix Biol. 78−79 (2019) 284−291.

[11] M. Aikio, H. Elamaa, D. Vicente, et al., Specific collagen XVIII isoforms promote adipose tissue accrual via mechanisms determining adipocyte number and affect fat deposition, Proc. Natl. Acad. Sci. 111 (2014) E3043−E3052.

[12] S.-Z. Chen, L.-F. Ning, X. Xu, et al., The miR-181d-regulated metalloproteinase Adamts1 enzymatically impairs adipogenesis via ECM remodeling, Cell Death Differ. 23 (2016) 1778−1791.

[13] T. Khan, E.S. Muise, P. Iyengar, et al., Metabolic dysregulation and adipose tissue fibrosis: role of collagen VI, Mol. Cell. Biol. 29 (2009) 1575−1591.

[14] S.R. Lamandé, J.F. Bateman, Collagen VI disorders: insights on form and function in the extracellular matrix and beyond, Matrix Biol. 71−72 (2018) 348−367.

[15] V.D. Myneni, A. Mousa, M.T. Kaartinen, Factor XIII-A transglutaminase deficient mice show signs of metabolically healthy obesity on high fat diet, Sci. Rep. 6 (2016) 35574.

[16] E.J. Hamson, F.M. Keane, S. Tholen, et al., Understanding fibroblast activation protein (FAP): substrates, activities, expression and targeting for cancer therapy, PROTEOMICS - Clin Appl 8 (2014) 454−463.

[17] E. Puré, R. Blomberg, Pro-tumorigenic roles of fibroblast activation protein in cancer: back to the basics, Oncogene 1 (2018).

[18] A.P. Marques, J. Cunha-Santos, H. Leal, et al., Dipeptidyl peptidase IV (DPP-IV) inhibition prevents fibrosis in adipose tissue of obese mice, Biochim Biophys Acta - Gen Subj 2018 (1862) 403−413.

[19] A. Subramanian, P. Tamayo, Mootha VK et al, A Knowledge-Based Approach for Interpreting Genome-Wide Expression Profiles, Gene Set Enrichment Analysis, 2005.

[20] A. Naba, K.R. Clauser, S. Hoersch, et al., The matrisome: in silico definition and in vivo characterization by proteomics of normal and tumor extracellular matrices, Mol. Cell. Proteomics 11 (2012) (M111.014647).

[21] S. Kidd, E. Spaeth, K. Watson, et al., Origins of the tumor microenvironment: quantitative assessment of adipose-derived and bone marrow-derived stroma, PLoS One 7 (2012), e30563.

[22] A. Ehrlund, J.R. Acosta, C. Björk, et al., The cell-type specific transcriptome in human adipose tissue and influence of obesity on adipocyte progenitors, Sci Data 4 (2017) 170164.

[23] D. Avery, P. Govindaraju, M. Jacob, et al., Extracellular matrix directs phenotypic heterogeneity of activated fibroblasts, Matrix Biol. 67 (2018) 90−106.

[24] X. Chen, O. Nadiarynkh, S. Plotnikov, et al., Second harmonic generation microscopy for quantitative analysis of collagen fibrillar structure, Nat. Protoc. 7 (2012) 654−669.

[25] M.-H. Fan, Q. Zhu, H.-H. Li, et al., Fibroblast activation protein (FAP) accelerates collagen degradation and clearance from lung in mice, J. Biol. Chem. 291 (2015) 8070−8089.

[26] K.E. Kadler, A. Hill, E.G. Canty-Laird, Collagen fibrillogenesis: fibronectin, integrins, and minor collagens as organizers and nucleators, Curr. Opin. Cell Biol. 20 (2008) 495−501.

[27] A. Carrer, J.L.D. Parris, S. Trefely, et al., Impact of a high-fat diet on tissue acyl-CoA and histone acetylation levels, J. Biol. Chem. 292 (2017) 3312−3322.

[28] M. Laplante, D.M. Sabatini, An emerging role of mTOR in lipid biosynthesis, Curr. Biol. 19 (2009) R1046−R1052.

[29] R. Aviram, S. Zaffryar-Eilot, D. Hubmacher, et al., Interactions between lysyl oxidases and ADAMTS proteins suggest a novel crosstalk between two extracellular matrix families, Matrix Biol. 75−76 (2019) 114−125.

[30] E.M. Morandi, R. Verstappen, M.E. Zwierzina, et al., ITGAV and ITGA5 diversely regulate proliferation and adipogenic differentiation of human adipose derived stem cells, Sci. Rep. 6 (2016) 28889.

[31] J. Heino, Cellular Signaling by Collagen-Binding Integrins, Springer, Dordrecht, 2014, pp. 143−155.

[32] K. Sun, J. Park, O.T. Gupta, et al., Endotrophin triggers adipose tissue fibrosis and metabolic dysfunction, Nat. Commun. 5 (2014) 3485.

[33] J.D. Knopf, S. Tholen, M.M. Koczorowska, et al., The stromal cell-surface protease fibroblast activation protein-α localizes to lipid rafts and is recruited to invadopodia, Biochim Biophys Acta - Mol Cell Res 2015 (1853) 2515−2525.

[34] A.-K. Picke, G.M. Campbell, M. Blüher, et al., Thy-1 (CD90) promotes bone formation and protects against obesity, Sci. Transl. Med. 1 (2018), https://doi.org/10.1126/scitranslmed.aao6806.

[35] J. Tchou, P.J. Zhang, Y. Bi, et al., Fibroblast activation protein expression by stromal cells and tumor-associated macrophages in human breast cancer, Hum. Pathol. 44 (2013) 2549−2557.

[36] Y. Luo, S. Ye, X. Chen, et al., Rush to the fire: FGF21 extinguishes metabolic stress, metaflammation and tissue damage, Cytokine Growth Factor Rev. (2017), https://doi.org/10.1016/j.cytogfr.2017.08.001.

[37] E.Y. Zhen, Z. Jin, B.L. Ackermann, et al., Circulating FGF21 proteolytic processing mediated by fibroblast activation protein, Biochem. J. 473 (2016) 605−614.

[38] D.R. Dunshee, T.W. Bainbridge, N.M. Kljavin, et al., Fibroblast activation protein cleaves and inactivates fibroblast growth factor 21, J. Biol. Chem. 291 (2016) 5986−5996.

[39] M.A. Sánchez-Garrido, K.M. Habegger, C. Clemmensen, et al., Fibroblast activation protein (FAP) as a novel metabolic target, Mol Metab 5 (2016) 1015−1024.

[40] B.L. Panaro, A.L. Coppage, J.L. Beaudry, et al., Fibroblast activation protein is dispensable for control of glucose homeostasis and body weight in mice, Mol Metab 19 (2019) 65−74.

[41] K. Subbaramaiah, L.R. Howe, P. Bhardwaj, et al., Obesity is associated with inflammation and elevated aromatase expression in the mouse mammary gland, Cancer Prev. Res. (Phila.) 4 (2011) 329−346.

[42] J. O'Connell, L. Lynch, A. Hogan, et al., Preadipocyte Factor-1 is associated with metabolic profile in severe obesity, J. Clin. Endocrinol. Metab. 96 (2011) E680−E684.

[43] T. McLaughlin, A. Sherman, P. Tsao, et al., Enhanced proportion of small adipose cells in insulin-resistant vs insulin-sensitive obese individuals implicates impaired adipogenesis, Diabetologia 50 (2007) 1707−1715.

[44] D. Klarin, S.M. Damrauer, K. Cho, et al., Genetics of blood lipids among ~300,000 multi-ethnic participants of the million veteran program, Nat. Genet. 50 (2018) 1514−1523.

[45] S. Onengut-Gumuscu, W.-M. Chen, O. Burren, et al., Fine mapping of type 1 diabetes susceptibility loci and evidence for colocalization of causal variants with lymphoid gene enhancers, Nat. Genet. 47 (2015) 381−386.